Food and Bioprocess Technology (2019) 12:2004–2017
https://doi.org/10.1007/s11947-019-02353-4

ORIGINAL PAPER

Microencapsulation of Microbial Transglutaminase by Ultrasonic Spray-Freeze Drying

Hilal Isleroglu[1] · Izzet Turker[1] · Banu Koc[2] · Mehmet Tokatli[1]

Received: 26 December 2018 / Accepted: 25 September 2019 / Published online: 2 November 2019
© Springer Science+Business Media, LLC, part of Springer Nature 2019

Abstract

Microencapsulation of partially purified microbial transglutaminase (mTG) was investigated using ultrasonic spray-freeze drying (USFD), and the optimum coating materials (gum arabic, maltodextrin, inulin) ratio and the process parameters (flow rate and nozzle frequency) were determined using a D-optimal combined design. Also, the microencapsulated samples by USFD were compared with microencapsulated samples by conventional freeze drying (CFD) and conventional spray drying (CSD) in terms of microencapsulation efficiency, enzyme stability at extreme pH and high temperature conditions, and the presence of metal ions, physical (moisture content, particle morphology, particle and pore size, surface area, pore volume distribution, density and flow properties, caking degree, color), and reconstitution (wettability and solubility) properties. As a result, the optimum coating materials composition was determined as 60% gum arabic and 40% inulin, and process conditions were found to be flow rate of 6.83 ml/min and nozzle frequency of 48 kHz applying desirability function method. Microcapsules with smaller particle size, pore volume, and porosity, with lower moisture content and good reconstitution characteristics, were obtained by USFD with a maximum microencapsulation efficiency of ~ 97%.

Keywords Ultrasonic spray-freeze drying · Transglutaminase · Inulin · Particle morphology · Pore volume distribution

Introduction

Microencapsulation is a technology offering the protection of foods and food components which are sensitive to external factors and processing conditions. It can be described as the incorporation of core bioactive compounds within coating material/several coating materials by different techniques (Desai and Park 2005). Several methods can be used for microencapsulation such as spray drying (SD), freeze drying (FD), solvent evaporation, gelation, fluidized bed coacervation, extrusion, and molecular inclusion (Aghbashlo et al. 2013; Nesterenko et al. 2013). Among these methods, SD is considered the most common method for the production of free flowing powders in huge quantities, being very compatible with different kinds of coating materials and having a low cost (Karthik and Anandharamakrishnan 2013). However, usage of high temperatures limits the applicability of the SD method for heat-sensitive bioactive materials such as enzymes (Sun-Waterhouse et al. 2013). Hence, FD, which is a low-temperature process, is more useful for heat labile materials and it is frequently used for the encapsulation of biomaterials (Heidebach et al. 2009; Amid et al. 2014; Amine et al. 2014). Powdered products having good rehydration properties can be obtained by FD due to the porous structures which are formed as a result of the sublimation of ice crystals during drying. However, FD has high operating costs owing to low-temperature and high-vacuum requirements and it is difficult to control particle size distribution of final products (Stapley 2008).

To overcome the limitations of SD and FD, spray-freeze drying (SFD) method, combining both processes, was developed (Ezhilarasi et al. 2013). SFD can be described as a three-

✉ Hilal Isleroglu
hilal.isleroglu@gop.edu.tr

Izzet Turker
izzet.turker@gop.edu.tr

Banu Koc
banukoc@gantep.edu.tr

Mehmet Tokatli
mehmet.tokatli@gop.edu.tr

[1] Faculty of Engineering and Natural Sciences, Department of Food Engineering, Tokat Gaziosmanpasa University, 60150 Tokat, Turkey

[2] Fine Arts, Gastronomy and Culinary Arts, Gaziantep University, 27310 Gaziantep, Turkey

step process involving atomization of the bulk solution/liquid, freezing of the atomized droplets by contacting to cryogenic fluid, followed by sublimation at low temperature and pressure (Ishwarya et al. 2015; Wanning et al. 2015). The fine droplets generated by atomization enable high heat transfer rates during spray-freezing step; thus, uniform formation of fine ice crystals can be achieved. The reduced product dimension provides enhanced sublimation rates and total drying time is reduced (MacLeod et al. 2006). Since the freezing and freeze-drying steps do not significantly alter the size of the droplet, the droplet size distribution obtained during atomization determines the particle size distribution of the final product. In addition to the hydraulic and pneumatic nozzles used in the SFD process, four-fluid nozzles and ultrasonic nozzles have been used in the drying of pharmaceutical products in recent years (Ishwarya et al. 2015). Ultrasonic nozzles that enhance the particle properties and ensure narrower particle size distribution of the product can operate at different frequencies. The size of droplets is controlled by the frequency and in general high-frequency nozzles produce smaller droplets (D'Addio et al. 2012). Although the use of the SFD for the purpose of microencapsulation is relatively new, it has been reported to be highly successful in terms of microencapsulation efficiency and protection of the core material (Kumar and Kar 2014). The SFD technique has been successfully applied for the microencapsulation of docosahexaenoic acid (Karthik and Anandharamakrishnan 2013), vitamin E (Parthasarathi and Anandharamakrishnan 2016), fish oil (Pang et al. 2017), vanillin (Hundre et al. 2015), *Lactobacillus paracasei* (Semyonov et al. 2010), *Lactobacillus plantarum* (Dolly et al. 2011; Rajam and Anandharamakrishnan 2015), and *Lactobacillus casei* (Her et al. 2015).

Proteins are one of the most important components of food products and modification of the food proteins can provide to obtain novel products and can improve the functional properties by chemical, physical, or enzymatic methods (Gaspar and Góes-Favoni 2015). In this regard, microbial transglutaminase (mTG) is the most effective enzyme which can modify functional properties of proteins by acyl transfer reactions, deamidation of protein-bound glutamines, and cross-linking glutamine and lysine peptide residuals (Motoki and Seguro 1998; Zhang et al. 2009; Popović et al. 2013). The mTG can alter the mechanical and textural properties of meat, dairy, and bakery products due to its cross-linking properties. Although the mTG can be widely used for different food products, there have been no reports regarding the preservation of the enzyme against environmental conditions through microencapsulation. The microencapsulation of the enzyme could prevent the alteration or destruction of its natural morphology, which causes a decrease in the activity and stability during the freeze drying process as well as the storage time until required in the industry (Amid et al. 2014).

In this study, the partially purified mTG, obtained from the batch fermentation of *S.mobaraensis*, was microencapsulated by ultrasonic spray-freeze drying (USFD) using gum arabic, maltodextrin, and inulin as coating materials. The D-optimal combined design was developed to determine the effects of coating materials ratio and process parameters (flow rate and nozzle frequency) on the enzyme activity. Also, the USFD method was compared with other two conventional methods (FD and SD) in terms of microencapsulation efficiency, enzyme stability in the presence of metal ions, extreme pH and high temperature, and physical and reconstitution properties.

Materials and Methods

Materials

Production of the mTG was carried out by batch fermentation of *Streptomyces mobaraensis* (NRRL B-3729) provided from the United States Department of Agriculture (USDA). A medium (initial pH value 6.0) containing whey (1000 ml) and molasses (30 g), that were obtained from commercial companies in Tokat, Turkey, as industrial food wastes, was used in the fermentation processes. Ammonium sulfate (Tekkim Chemicals, extra pure) and dialysis tubing cellulose membrane (Sigma-Aldrich, ~flat width 76 mm, 14 kDa molecular weight cut-off) were used for the partial purification of mTG. The Z-Gln-Gly as a donor substrate and -glutamic acid γ-monohydroxamate as a standard for calibration curve were obtained from Sigma Chemical Co., Ltd. Commercial forms of gum arabic, maltodextrin (DE 20), and inulin were used as coating materials for the microencapsulation process.

Preparation of Feed Solutions

Production and partial purification of the mTG was carried out according to Isleroglu et al. (2018). After batch fermentation (in the flasks for 4 days at 30 °C of incubation temperature and 150 rpm of shaking rate) and partial purification of the mTG using ammonium sulfate (saturation of 80%) precipitation, the precipitated particles were collected and subjected to dialysis to obtain the crude enzyme solution. The dialysis process was ended when the dry matter content of the solution was reduced to ~ 10% which was determined by using an infrared moisture analyzer; thus, the crude enzyme solution was obtained.

Maltodextrin, gum arabic, and inulin were dissolved in water (10%, w/w) one night before the microencapsulation processes and kept at 4 °C for rehydration. The ratio of dry matter enzyme solution to coating material was fixed at 1:2 for all runs. The calculated amount of coating materials from experimental design (Table 1) was homogenized for 5 min at 11200 rpm using a rotor-stator homogenizer (Ultra-Turrax IKA T-18 Basic, USA). After homogenization of the coating

Table 1 Microencapsulation efficiency (ME) and relative activity values (%) of USFD process

Flow rate (ml/min)	Nozzle frequency (kHz)	Gum arabic (%)	Maltodextrin (%)	Inulin (%)	Relative activity after freezing (%)	Relative activity after drying (%)	ME (%)
2.0	48	35	35	30	102.54 (± 0.30)	89.07 (± 0.02)	91.60 (± 0.02)
8.0	48	100	0	0	104.01 (± 0.27)	86.62 (± 0.50)	90.09 (± 0.52)
2.0	120	40	0	60	102.22 (± 1.11)	91.97 (± 0.37)	94.01 (± 0.38)
8.0	120	50	50	0	107.57 (± 0.75)	82.32 (± 0.70)	88.55 (± 0.75)
5.0	48	100	0	0	105.03 (± 0.27)	84.54 (± 0.02)	88.79 (± 0.02)
8.0	48	50	50	0	106.47 (± 0.40)	84.28 (± 0.08)	89.74 (± 0.08)
2.0	48	40	0	60	102.81 (± 0.28)	93.11 (± 0.41)	95.73 (± 0.42)
8.0	120	0	100	0	101.98 (± 0.40)	86.86 (± 0.33)	88.58 (± 0.34)
6.5	48	70	0	30	102.61 (± 0.28)	90.42 (± 0.04)	92.78 (± 0.04)
8.0	120	40	0	60	102.70 (± 0.32)	94.01 (± 0.14)	96.55 (± 0.14)
5.0	120	0	100	0	103.88 (± 0.20)	85.54 (± 0.10)	88.86 (± 0.10)
5.0	120	100	0	0	105.16 (± 0.40)	86.08 (± 0.06)	90.53 (± 0.06)
5.0	48	35	35	30	103.21 (± 0.40)	89.67 (± 0.23)	92.55 (± 0.24)
2.0	120	0	100	0	105.66 (± 0.20)	83.09 (± 0.40)	86.39 (± 0.43)
8.0	48	40	0	60	103.13 (± 0.16)	93.12 (± 0.02)	96.04 (± 0.02)
8.0	120	35	35	30	103.82 (± 0.40)	88.11 (± 0.27)	91.48 (± 0.28)
5.0	120	0	40	60	103.58 (± 0.16)	90.52 (± 0.12)	93.76 (± 0.12)
8.0	48	35	35	30	103.57 (± 0.16)	89.58 (± 0.27)	92.78 (± 0.27)
8.0	48	40	0	60	104.13 (± 0.45)	93.25 (± 0.16)	97.10 (± 0.16)
2.0	48	0	40	60	103.75 (± 0.39)	90.24 (± 0.25)	93.63 (± 0.26)
8.0	120	50	50	0	105.01 (± 0.24)	84.00 (± 0.13)	88.64 (± 0.14)
2.0	120	35	35	30	105.92 (± 0.59)	85.53 (± 0.36)	90.60 (± 0.38)
2.0	120	100	0	0	104.62 (± 0.40)	85.55 (± 0.29)	89.51 (± 0.30)
5.0	120	50	50	0	104.63 (± 0.32)	84.34 (± 0.23)	88.25 (± 0.24)
2.0	48	0	100	0	103.73 (± 0.16)	83.28 (± 0.14)	87.80 (± 0.14)
8.0	48	0	100	0	103.52 (± 0.24)	84.45 (± 0.14)	87.42 (± 0.14)
8.0	120	100	0	0	104.78 (± 0.44)	87.35 (± 0.13)	91.53 (± 0.14)
8.0	48	0	40	60	103.69 (± 0.12)	90.76 (± 0.10)	94.11 (± 0.10)
2.0	48	40	0	60	103.26 (± 0.36)	91.97 (± 0.27)	94.97 (± 0.28)
3.5	120	70	0	30	102.31 (± 0.23)	90.41 (± 0.25)	92.50 (± 0.25)
2.0	48	50	50	0	103.00 (± 0.08)	86.32 (± 0.14)	88.91 (± 0.14)
3.5	48	70	0	30	102.92 (± 0.24)	89.26 (± 0.08)	91.86 (± 0.08)
8.0	120	40	0	60	103.77 (± 0.76)	93.11 (± 0.00)	96.63 (± 0.00)
2.0	120	50	50	0	103.39 (± 0.16)	85.15 (± 0.08)	88.04 (± 0.08)
5.0	48	0	100	0	103.81 (± 0.04)	83.34 (± 0.11)	86.51 (± 0.11)
2.0	48	100	0	0	104.54 (± 0.43)	83.05 (± 0.34)	86.82 (± 0.36)
5.0	48	40	0	60	101.96 (± 0.44)	94.70 (± 0.12)	96.56 (± 0.12)
2.0	120	0	40	60	103.34 (± 0.56)	89.56 (± 0.10)	92.55 (± 0.10)
8.0	120	0	40	60	103.57 (± 0.16)	91.17 (± 0.10)	94.43 (± 0.10)
8.0	120	0	40	60	103.69 (± 0.24)	90.98 (± 0.06)	94.34 (± 0.06)

materials mixture, the crude enzyme solution was mixed with the prepared coating materials to achieve a total dry matter content of 10%. The resulting mixture containing crude enzyme and coating materials were homogenized once more for 5 min at 11200 rpm to achieve the feed solution.

Microencapsulation by Ultrasonic Spray-Freeze Drying Process

The microencapsulation of the mTG by USFD process was carried out using the system described in Isleroglu et al.

(2018). The feed solution was fed with a syringe pump (Syringe Pump TI, SonoTek Inc., USA) at different flow rates (2–8 ml/min) and was atomized by ultrasonic nozzles (SonoTek Inc., USA) operating at two different frequencies (48 kHz and 120 kHz) using an ultrasonic generator (ECHO, SonoTek Inc., USA). The atomized fine droplets were frozen using liquid nitrogen. A distance of 7 cm was kept constant between the ultrasonic nozzle and liquid nitrogen surface, and the stainless steel liquid nitrogen container was stirred with a magnetic agitator constantly to prevent clumping of the particles. Approximately 50 ml of feed solution was atomized for each run. After freezing, the excess liquid nitrogen was subsequently removed from the slurry by evaporation, and the resulting pellet containing the frozen droplets was transferred to a pre-cooled shelf (~ − 35 °C) of a freeze dryer (CHRIST, Alpha 1-4 LSC, Germany). The frozen particles were subjected to main drying for 12 h at 1 mbar, and then to secondary drying for 4 h with a shelf temperature at 30 °C under a vacuum of 0.01 mbar. Also, the partially purified crude enzyme solution was dried by USFD without coating materials to demonstrate the effect of microencapsulation and the obtained samples called as USFD-CE.

Determination of Microencapsulation Efficiency and Experimental Design

The microencapsulation efficiency (ME, %) was defined as the enzyme activity of the final product over the initial activity of the feed solution (Eq. 1). The mTG activity was determined using the colorimetric hydroxamate method with the specific substrate of Z-Gln-Gly (Turker et al. 2016; Isleroglu et al. 2018). One unit of mTG activity in 1 ml of sample (U/ml) was described as the amount of enzyme that caused the formation of 1.0 μmole of hydroxamate per minute by catalyzing the reaction between Z-Gln-Gly and hydroxylamine at pH 6.0 and 37 °C (Bourneow et al. 2012)

$$\mathrm{ME}\ (\%) = \frac{\textit{Activity of the final product}\ (\mathrm{U/ml})}{\textit{Activity of initial feed solution}\ (\mathrm{U/ml})} \times 100 \qquad (1)$$

Moreover, to determine the effects of atomizing-freezing and the freeze-drying steps on the enzyme activity during USFD process, Eq. 2 and Eq. 3 were used, respectively.

$$\textit{Relative activity after freezing}\ (\%) = \frac{\textit{Activity after freezing}\ (\mathrm{U/ml})}{\textit{Activity of initial feed solution}\ (\mathrm{U/ml})} \times 100 \qquad (2)$$

$$\textit{Relative activity after drying}\ (\%) = \frac{\textit{Activity of the final product}\ (\mathrm{U/ml})}{\textit{Activity after freezing}\ (\mathrm{U/ml})} \times 100 \qquad (3)$$

A D-optimal combined design was performed to investigate the effects of the coating materials mixture and process variables on microencapsulation efficiency during USFD (Table 1). A combined design, combination of mixture components and process factors, was used to optimize the coating material composition and processing parameters. Gum arabic, maltodextrin, and inulin ratio; flow rate; and nozzle frequency were selected as independent mixture and process variables, respectively, and experimental design including 40 runs was given in Table 1. All experimental data was fitted to a second-order polynomial model and the optimum mixture and process conditions providing the maximum microencapsulation efficiency were estimated using the desirability function method.

Conventional Freeze-Drying and Spray-Drying Process

As a result of the optimization process, the feed solution prepared with ratios determined for the coating materials was frozen at − 80 °C for 4 h without atomization and transferred to a pre-cooled shelf (~ − 35 °C) of the freeze dryer. The same drying conditions used in the USFD (12 h of main drying + 4 h of secondary drying) were also carried out for the CFD process. Furthermore, the same feed solution was dried using a spray dryer (Büchi Mini Spray Dryer B-290, Switzerland) with a determined flow rate at the optimum point of USFD. The inlet-outlet temperatures were 150 °C and 79 °C for CSD, respectively.

Analyses

Effects of Different Metal Ions, Extreme pH, and High Temperature

The relative activities of the four different types of powders obtained from different drying operations (USFD-CE, USFD, CFD and CSD) were investigated in the presence of different metal ions (EDTA.$2H_2O$, $ZnSO_4.7H_2O$, $FeCl_3.6H_2O$, $CaCl_2.XH_2O$, and $CoCl_2.6H_2O$). Furthermore, the effects of extreme pH (3.0 and 8.0) and temperature (80 °C) on the enzyme activity were evaluated and the relative activity was calculated as a percentage of activity remaining after incubation at mentioned conditions (presence of reagents, at different pH levels and/or high temperature) to the activity of final product. The details about the procedure were given in Isleroglu et al. (2018).

Physical Properties

Moisture Content The moisture content of the powder samples was determined using an infrared moisture analyzer (Shimadzu, MOC 63u, Japan) at 90 °C and the results were validated by the standard oven method (AOAC 1990).

Water Activity The values of water activity in powder samples were measured using a water activity measurement device (Aqualab 3 TE, USA).

Particle Morphology The particle morphology of four different types of powders (USFD-CE, USFD, CFD, and CSD) was determined using scanning electron microscopy (SEM) (Zeiss Evo LS 10, Germany). Samples were placed onto aluminum stages using adhesive carbon conducting tape and the particles were coated with gold for 200 s. The accelerating voltage for scanning was 20 kV, and vacuum was applied at 9.75×10^{-5} torr.

Particle Size Analysis The particle size distribution of the four different types of powders (USFD-CE, USFD, CFD, and CSD) was measured using a laser light diffraction particle size analyzer (Malvern Mastersizer 2000, UK). Analyses were done in five successive trials and data was reported as average. The particle size of the samples was expressed as $D_{4,3}$ (mean volumetric size, Eq. 4), and the particle size distribution of the powder was measured as the span (Eq. 5).Equation ID=t=t

$$D_{4,3} = \frac{\sum n_i d_i^4}{\sum n_i d_i^3} \tag{4}$$

$$span = \frac{d_{90} - d_{10}}{d_{50}} \tag{5}$$

where, n_i is the number of particles having diameters d_i; d_{90}, d_{10}, and d_{50} are the equivalent volume diameters at cumulative volumes of 90, 10, and 50%, respectively.

Surface Area and Pore Volume Analysis The N_2 adsorption-desorption isotherms of four different types of powders (USFD-CE, USFD, CFD, and CSD) were obtained under relative pressures (P/P_0) ranging from 0.01 to 1 at 77 K (Autosorb 6-B, Quantachrome Corp., USA). The surface area (m^2/g), pore volume (cm^3/g), and pore size (nm) of the samples were determined using BJH (Barrett-Joyner-Halenda) method. Prior to the measurements, the samples were degassed at 40 °C for 16 h.

Density and Flow Properties The particle (ρ_p), bulk (ρ_b), and tapped (ρ_t) densities, and the porosity (ε) of four different types of samples (USFD-CE, USFD, CFD, and CSD) were determined according to Isleroglu et al. (2018). Also, the flowing behavior of the samples was stated in terms of the Carr index (CI) and Hausner ratio (HR), and they were calculated using Eq. 6 and Eq. 7, respectively (Carr 1965; Hausner 1967).Equation ID=t=t

$$\mathrm{CI} = {}^{(\rho_t - \rho_b)}\Big/_{\rho_t} \times 100 \tag{6}$$

$$\mathrm{HI} = {}^{\rho_t}\Big/_{\rho_b} \times 100 \tag{7}$$

According to Carr (1965), the flowing behavior of powders is classified as very poor, poor, fair, good, and very good for CI values greater than 45, 35–45, 20–35, and 15–20 and less than 15, respectively. The flowability is defined as good where the HR value is less than 1.2, it is medium between 1.2 and 1.4, and poor if greater than 1.4 (Hausner 1967).

Caking Degree The caking degree of four different types of samples (USFD-CE, USFD, CFD, and CSD) was determined according to Isleroglu et al. (2018) and calculated by Eq. 8.

$$Caking\ degree\ (\%) = \frac{(100 \times b)}{a} \tag{8}$$

where, a is the amount of the sample (g) and b is the amount of powder (g) remaining in the sieve.

Color Measurement The color measurements of four different types of samples (USFD-CE, USFD, CFD, and CSD) were carried out with a 3NH Colorimeter NR-200 (Chinese), and CIE L^* (lightness), a^* (redness), and b^* (yellowness) values were detected.

Reconstitution Properties

Wettability The wettability test of the samples was determined using a system comprising a beaker and a glass funnel. The glass funnel was clamped at a height of 10 cm from the 250 ml beaker, which contained 100 ml of water. A glass test tube was placed inside the funnel and the powder sample (0.1 g) was located around the test tube. The tube was lifted while the stop watch was started at the same time and the time was recorded when the powder became completely wetted (Jinapong et al. 2008).

Solubility One gram of the sample was diluted in 25 ml of distilled water and was stirred for 15 min at 3000 rpm with a magnetic stirrer to analyze solubility. The resulting mixture was placed in Eppendorf tubes and centrifuged at 3000 rpm for 5 min. After centrifugation, the supernatant was transferred to metal drying plates and dried in an oven at 105 ± 2 °C for 4 h. The solubility (%) was calculated by the weight difference (mass after drying/initial mass) (Cano-Chauca et al. 2005).

Statistical Analysis

The significant terms in the models, which described the effects of the coating materials mixture (gum arabic (C_1), maltodextrin (C_2), inulin (C_3)), and process variables (flow rate (X_1) and nozzle frequency (X_2)) on microencapsulation efficiency during USFD, were found through the analysis of variance (ANOVA) by using the software (Design Expert-version 7.0 Stat-Ease Inc., USA). The model for microencapsulation efficiency

created for regression analysis of the obtained data was given by Eq. 9.

$$\mathrm{ME}\ (\%) = \beta_0 + \sum_{i=1}^{k} \beta_i X_i + \sum_{i=1}^{k} \beta_i X_i^2 + \sum_{i=1}^{k-1} \sum_{j=1+1}^{k} \beta_{ij} X_{ij} \quad k = 1 \quad (9)$$

Two experiments were achieved at the estimated optimum conditions, that provide the maximum microencapsulation efficiency, and one sample t test was performed to verify the optimization. The relative activity results and physical properties obtained by different microencapsulation methods (extreme pH, high temperature, presence of metal ions) were analyzed using SPSS 22.0 statistics package program (IBM Corp., New York, NY) and the data was evaluated using a Duncan significant difference test at a confidence level of $p < 0.05$.

Results and Discussion

The experimental relative activity values obtained according to D-optimal design (Table 1) were evaluated for microencapsulation efficiency (%) to determine the optimum composition of coating materials (gum arabic, maltodextrin, inulin) and optimum process conditions (flow rate (m/s) and nozzle frequency (kHz)). When the relative activity values after freezing were investigated, it was observed that the enzyme activity increased at all conditions regardless of the type of coating material and process conditions. This phenomenon indicated that the ultrasonic atomization and freezing steps did not damage the structural configuration of mTG; to the contrary, activity was affected in a positive manner. Small ice crystals were formed due to the rapid freezing of small droplets generated by the ultrasonic atomization. The conformational changes that occur in the tertiary structure of the enzyme as a result of these small ice crystals may enhance the activity (Breda et al. 1992). Furthermore, the atomizing process that promotes small droplets may lead to accessibility to the enzyme surface for the substrate, and so the measured relative activity after freezing was increased.

The relative activity values after drying are also given in Table 1 to represent the effect of drying step on the enzyme activity. The results clearly showed that the reduction in enzyme activity mainly caused by the drying step. Although the freeze-drying process is a suitable method for heat-sensitive components, it can cause different types of stresses such as low-temperature stress, dehydration stress, and ice crystal formation which can deactivate and destabilize the enzymes (Ramos et al. 1997). Isleroglu et al. (2018) revealed that the activity loss of mTG occurred in the drying step of USFD, while the enzyme activity was enhanced by ultrasonic atomizing, and they recommended further researches to preserve the enzyme activity during the drying step. According to the results, the relative activities after drying were maintained over 90% where the ratio of inulin was 60% in the mixture of coating materials. On the contrary, the lowest relative activity values (~ 84%) were obtained when the maltodextrin ratio was high (Table 1). Desai and Park (2005) indicated that the structure of the carbohydrate may affect the encapsulation yield of final products containing proteins. Accordingly, one of the most possible reasons of different behaviors of coating materials can be the linking properties of carbohydrates with protein (enzyme) molecules. When proteins are subjected to freezing and drying processes, they lose their hydration shells and that phenomenon may cause the formation of intramolecular hydrogen bonds within proteins which may change their tertiary structure (Carpenter and Crowe 1989; Allison et al. 1999; Anchordoquy et al. 2001). If carbohydrates are added before drying, the hydrogen bonds between protein and hydroxyl groups of carbohydrates take place of the hydrogen bonds between protein molecules and water. This mechanism provides preserving the tertiary structure of protein molecules (Tonnis et al. 2015). The polysaccharides such as maltodextrin may interact with protein molecules but they may leave some open gaps on the interaction surface. However, inulin, which is composed of flexible furanose groups and has a backbone composed of polyethylene oxide giving the molecule greater freedom and flexibility, can cover an enzyme molecule tighter than a rigid protein-maltodextrin matrix and preserve the mTG activity much better. In literature, the success of inulin as an effective protein-protector for freze-drying operations has been explained in several studies (Eriksson et al. 2002; Furlán et al. 2012; Grasmeijer et al. 2013; Tonnis et al. 2014).

The microencapsulation efficiency (ME, %) values, which indicate the relative activity after USFD, are also given in Table 1. According to the results, the lowest ME (86.39%) occurred at a 2.0 ml/min flow rate, 120 kHz nozzle frequency, and 100% maltodextrin concentration. On the other hand, the highest ME (97.1%) was obtained at an 8.0 ml/min flow rate, 48 kHz nozzle frequency, and the mixture of gum arabic and inulin with the ratios of 40% and 60%, respectively. When the process parameters (flow rate and nozzle frequency) were examined, it was observed that the ME (%) increased at increasing flow rates, and decreased when the 120 kHz nozzle frequency was used (Table 1). Ultrasonication can cause mechanical stress developed by eddies arising from ultrasound waves in the nozzle and this mechanical stress can affect the enzymes inversely (Feng et al. 2011). When the frequency to flow rate ratio was high, ultrasonic vibrational energy which created more mechanical stress on the enzyme molecule increased and caused lower relative activity values.

The statistical analysis of the effect of independent variables on ME (%) is shown in Table 2. The results showed that the regression model was statistically significant at 99% confidence level ($p < 0.01$). The lack of fit value for the generated model was not statistically significant ($p > 0.05$). Moreover, the

Table 2 ANOVA results of optimization process in terms of microencapsulation efficiency

Variation source	SD	Coefficient	Sum of squares	*F* value	*p* value
Model	29	-	386.8003	83.588	< 0.0001
Linear mixture	2	-	349.2797	1094.453	< 0.0001
C_1C_2	1	1.32	0.0879	0.551	0.475
C_1C_3	1	− 1.11	0.0133	0.083	0.7788
C_1X_1	1	1.31	6.9782	43.732	< 0.0001
C_1X_2	1	1.01	6.3209	39.612	< 0.0001
C_2C_3	1	− 6.07	0.2624	1.644	0.2287
C_2X_1	1	0.45	0.8141	5.102	0.0475
C_2X_2	1	0.82	4.0754	25.540	0.0005
C_3X_1	1	1.14	0.2002	1.255	0.2888
C_3X_2	1	− 0.58	0.0673	0.422	0.5308
$C_1C_2X_1$	1	− 2.03	0.7818	4.900	0.0513
$C_1C_2X_2$	1	− 5.98	8.5537	53.605	< 0.0001
$C_1C_3X_1$	1	− 1.09	0.0328	0.205	0.6602
$C_1C_3X_2$	1	− 1.58	0.0959	0.601	0.4561
$C_1X_1X_2$	1	− 0.30	0.3675	2.303	0.1601
$C_2C_3X_1$	1	− 1.09	0.0321	0.201	0.6632
$C_2C_3X_2$	1	− 1.05	0.0373	0.234	0.6391
$C_2X_1X_2$	1	− 0.06	0.0143	0.090	0.7706
$C_3X_1X_2$	1	1.47	0.3350	2.099	0.178
$C_1X_1^2$	1	− 0.12	0.0198	0.124	0.7321
$C_2X_1^2$	1	− 0.13	0.0216	0.135	0.7205
$C_3X_1^2$	1	− 1.47	0.0678	0.425	0.5291
$C_1C_2X_1X_2$	1	0.42	0.0343	0.215	0.6528
$C_1C_3X_1X_2$	1	− 1.74	0.0829	0.519	0.4876
$C_2C_3X_1X_2$	1	− 2.19	0.1302	0.816	0.3876
$C_1C_2X_1^2$	1	0.00	2.33×10^{-8}	1.46×10^{-7}	0.9997
$C_1C_3X_1^2$	1	1.84	0.0224	0.140	0.7159
$C_2C_3X_1^2$	1	1.94	0.0199	0.124	0.7316
Residual	10		1.5957		
Lack of fit	5		0.7396		0.5618
Pure error	5		0.8560		
Total	39		388.3960		
R^2	0.9959				
Adj-R^2	0.9840				
Adeq. Precision	30.006				
PRESS	57.28				
C.V. (%)	0.44				

C_1 gum arabic (%), C_2 maltodextrin (%), C_3 inulin (%), X_1 flow rate (ml/min), X_2 nozzle frequency (kHz)

R^2 value, which indicates the ratio of the variation explained by the model, was calculated as 0.9959 and it was determined that the major part of the variation could be explained by the model. The adj-R^2 value was also calculated as 0.9840, which indicated that there were no insignificant terms in model. The C.V. (%) value was quite low (0.44%) establishing that experimental values were very close to the mean values. The Adeq. Precision value higher than 4 and low PRESS values of the model showed that the model is suitable for precision of the relative activity values. The polynomial model obtained for determination of ME (%) was given as coded factors in Eq. 10.

$$\mathrm{ME}\ (\%) = +89.60C_1 + 87.67C_2 + 100.90C_3 + 1.31C_1X_1 + 1.01C_1X_2 + 0.82C_2X_2 - 5.98C_1C_2X_2 \quad (10)$$

When a desirability function approach was applied, the optimum USFD process conditions were determined as 6.83 ml/min of flow rate and 48 kHz of nozzle frequency; and optimum mixture composition was determined as 40% of gum arabic and 60% of inulin. The ME (%) was predicted as 96.62% at these optimum conditions. To validate the optimum USFD conditions, three experiments were performed, and the experimental (96.96 ± 0.48%) and predicted ME (%) values were compared according to the *t* test. No significant difference was determined between the predicted and experimental values ($p > 0.05$).

The samples produced by conventional microencapsulation techniques (CFD and CSD) using optimum coating materials ratios (60% gum arabic, 40% inulin) were compared with the samples microencapsulated by USFD in terms of microencapsulation efficiency and relative activity values at different conditions and the results are given in Table 3. The highest relative activity value after microencapsulation (microencapsulation efficiency) for different drying processes was obtained by USFD ($p < 0.05$). The remaining activity values were listed as USFD>CFD>CSD among the microencapsulated samples and in the USFD-CE sample obtained at the optimum process conditions (flow rate 6.83 ml/min and nozzle frequency 48 kHz), and the remaining activity value was found to be lower than all microencapsulated samples ($p < 0.05$) (Table 3). This result clearly revealed the positive effect of the microencapsulation process for preserving the activity of mTG. The presence of coating materials in the environment reduced the loss of activity even if different methods were used. Longer freezing time of CFD process than USFD caused more stress on mTG; hence, the relative activity values were found to be lower than USFD. Also, larger ice crystals generated as a result of slow freezing damaged the enzyme molecules during sublimation (Ishwarya et al. 2015). Similarly, in a study that produced powdered tetrahydrocannabinol (THC) by SFD and CFD using inulin as a coating material, a more stable form of THC was obtained by the SFD process rather than the CFD (van Drooge et al. 2005). According to comparison results, it was also observed that the CSD samples had the lowest relative activity values among microencapsulated counterparts and this situation could be explained by the high temperature used during

Table 3 Relative activity values of crude and microencapsulated enzymes by different methods

Condition	Relative activity (%)			
	USFD-CE	USFD	CFD	CSD
After process	65.08 (±0.18)^{a}	96.96 (±0.48)^{b}	79.26 (±0.14)^{c}	73.09 (±0.29)^{d}
pH 3.0	74.93 (±0.47)^{a}	88.00 (±0.60)^{b}	84.59 (±0.78)^{c}	76.19 (±0.87)^{a}
pH 8.0	35.20 (±0.06)^{a}	49.51 (±0.74)^{b}	49.95 (±2.88)^{b}	45.91 (±0.73)^{b}
80 °C	12.59 (±0.03)^{a}	18.26 (±0.56)^{b}	16.40 (±0.10)^{c}	13.03 (±0.13)^{a}
EDTA	114.36 (±1.16)^{a}	107.72 (±0.28)^{b}	110.05 (±0.45)^{c}	111.40 (±0.33)^{c}
Fe^{2+}	43.98 (±0.40)^{a}	68.38 (±2.21)^{b}	60.87 (±0.08)^{c}	43.38 (±0.40)^{a}
Ca^{2+}	84.84 (±0.47)^{ab}	87.37 (±1.25)^{c}	82.85 (±0.10)^{a}	86.26 (±0.13)^{bc}
Co^{2+}	57.60 (±0.07)^{a}	57.66 (±0.49)^{a}	53.17 (±0.57)^{b}	50.18 (±0.47)^{c}
Zn^{2+}	nd	nd	nd	nd

nd not determined

$^{a–d}$ The mean values on the same line having different superscripts are significantly different ($p < 0.05$)

CSD process (Ratti 2001; Mujumdar 2014). Although the comparison studies of different microencapsulation methods including SFD are limited, the current results are in accordance with the studies of Karthik and Anandharamakrishnan (2013), Ishwarya and Anandharamakrishnan (2015), and Parthasarathi and Anandharamakrishnan (2016).

The relative activities at different pH values and high temperature of different samples were also determined (Table 3). The USFD samples showed the highest activity at pH 3.0 and 80 °C ($p < 0.05$). However, when the pH value was 8.0, the relative activities of microencapsulated samples was not differentiated significantly ($p > 0.05$) due to approaching the isoelectric point of pH 8.9 (Bourneow et al. 2012). Nevertheless, all microencapsulated samples showed higher relative activity at pH 8.0 than USFD-CE, which could be explained by the protective effect of the coating materials. EDTA, which is a chelating agent, had an increasing effect on relative activity for all samples due to making complexes with the metal ions present on the active site of mTG (Table 3). The fact that the USFD-CE samples did not contain any coating material caused EDTA to show the chelating effect better than microencapsulated samples and the highest activity values were obtained for USFD-CE samples ($p < 0.05$). When Fe^{2+}, Ca^{2+}, and Co^{2+} were present in the assay medium, the relative activity values were decreased, and Zn^{2+} inhibited mTG activity in all samples (Table 3).

The physical and reconstitution properties of the samples were compared and the results are given in Table 4. According to the moisture and water activity results, all samples were statistically different in terms of moisture and water activity values ($p < 0.05$), and the lowest values were obtained in the CSD samples due to the application of high temperature (Table 4). Small ice crystals were formed with the increase in nucleation rate during the USFD process, and the droplets with small ice crystals increased the heat and mass transfer coefficients, resulting in lower moisture content at the end of the drying process. The samples having a lower moisture content obtained by USFD showed that the USFD process can be applied with shorter drying times, and therefore, it will be a more cost-effective process than CFD. When the bulk and tapped density values were considered, the highest values were obtained in USFD and CFD samples while the lowest values were obtained in USFD-CE and CSD samples (Table 4). It was thought that the low bulk density values of the USFD-CE and CSD samples were related to their smaller particle size compared with USFD and CFD samples. Although the particle density values were found to be close to each other in all samples, the samples microencapsulated by USFD and CFD were found to be lower than the particle density of USFD-CE and CSD samples ($p < 0.05$). As the highest porosity values were obtained for the USFD-CE and CSD samples ($p < 0.05$), the USFD and CFD had similar porosity values ($p > 0.05$). While the caking degree was low in USFD-CE, USFD, and CFD samples, it was determined that the caking degree values were higher than 70% in the microencapsulated samples by CSD (Table 4). The agglomeration of very small particles formed in the CSD process caused the caking degree values to increase in the CSD samples. When the CI values of all the samples were examined, the flow properties were considered to be very poor (CI > 45); however, the microencapsulated samples by USFD were found to have medium flowability according to HR values (Table 4). In general, it is known that the wider particle size distribution affects the light transmittance of the materials, leading to a decrease in the color strength (Heinrich 2003). The low L^*, a^*, and b^* values of CFD samples supported this situation (Table 4). The good solubility of the coating materials used and the enzyme in the water allowed the solubility values obtained in all conditions to be quite high (> 95%). The term of wettability is water absorption capacity on the surface of the particle. It can characterize the dissolution properties of the powder and thus indicate how fast the enzyme exhibits

Table 4 Physical and reconstitution properties of crude and microencapsulated enzymes by different methods

Property	Sample			
	USFD-CE	USFD	CFD	CSD
Moisture (%)	4.94 (± 0.02)^{a}	5.19 (± 0.03)^{b}	5.89 (± 0.07)^{c}	4.50 (± 0.01)^{d}
a_w	0.199 (± 0.002)^{a}	0.293 (± 0.002)^{b}	0.378 (± 0.016)^{c}	0.113 (± 0.005)^{d}
BD (kg/m^3)	434.1 (± 2.9)^{a}	583.5 (± 8.8)^{b}	584.2 (± 4.8)^{b}	444.1 (± 18.2)^{a}
TD (kg/m^3)	555.5 (± 8.2)^{a}	728.3 (± 7.5)^{b}	773.0 (± 17.4)^{b}	666.2 (± 18.2)^{c}
PD (kg/m^3)	1454.8 (± 2.4)^{a}	1420.8 (± 10.2)^{b}	1429.9 (± 4.9)^{b}	1457.4 (± 10.7)^{a}
Porosity (%)	70.2 (± 0.1)^{a}	58.9 (± 0.8)^{b}	59.1 (± 0.4)^{b}	69.5 (± 0.2)^{a}
CI (%)	61.8 (± 0.5)^{a}	48.7 (± 0.4)^{b}	45.9 (± 1.4)^{b}	54.3 (± 1.5)^{c}
HR	1.28 (± 0.01)^{ab}	1.25 (± 0.03)^{b}	1.32 (± 0.03)^{a}	1.50 (± 0.03)^{c}
Caking degree (%)	34.5 (± 1.0)^{a}	35.9 (± 6.9)^{a}	35.2 (± 13.9)^{a}	74.7 (± 3.2)^{b}
L^*	56.3 (± 0.5)^{a}	58.4 (± 2.0)^{a}	44.8 (± 1.3)^{b}	81.7 (± 2.1)^{c}
a^*	11.7 (± 0.2)^{a}	11.7 (± 0.4)^{a}	3.6 (± 0.5)^{b}	5.8 (± 0.5)^{c}
b^*	26.8 (± 0.4)^{a}	27.0 (± 0.6)^{a}	10.1 (± 1.1)^{b}	16.1 (± 0.4)^{c}
$D_{[4,3]}$ (μm)	136.72 (± 5.74)^{a}	238.10 (± 25.59)^{b}	348.45 (± 32.54)^{c}	7.44 (± 0.08)^{d}
Span	1.49 (± 0.08)^{a}	4.23 (± 0.83)^{b}	6.94 (± 0.83)^{c}	1.87 (± 0.01)^{a}
Solubility (%)	95.5 (± 0.3)^{a}	96.2 (± 0.2)^{b}	96.6 (± 0.1)^{c}	96.6 (± 0.16)^{c}
Wettability (s)	14.0 (± 0.2)^{a}	3.2 (± 0.2)^{b}	11.1 (± 1.2)^{a}	26.9 (± 4.0)^{c}

All data are reported as means (± standard deviations) of at least 2 parallel measurements

BD bulk density, *TD* tapped density, *PD* particle density, *CI* Carr index, *HR* Hausner ratio, a_w water activity

$^{a–d}$ The mean values on the same line having different superscripts indicate that the means are statistically different ($p < 0.05$)

activity. When the wettability values were examined, it was determined that the microencapsulated samples with USFD could get wet faster than other samples (Table 4). The high wettability value obtained for the CSD samples was thought to result from the agglomerates formed by combining the small particles which prevented the contact of the individual particles with water.

Particle size and morphology in microencapsulated products are affected by the type of coating materials, the rheological properties of the feed solution, atomizing method, and drying conditions (Dima et al. 2016). Even if the same coating material is used, different microencapsulation methods result in different particle size and distribution in the final product which affect the physical and reconstitution properties (Parthasarathi and Anandharamakrishnan 2016). The mean volumetric particle size ($D_{[4,3]}$) and span values are given in Table 4 and the particle size distribution of the samples are illustrated in Fig. 1. It was determined that the samples with the lowest particle size were obtained by CSD method, while the samples with the highest particle size were obtained by microencapsulation by CFD (Table 4). Although preventing over particle size has the advantage of reducing drying times, very small particle size of CSD samples can enhance total particle surface area which may led to agglomeration by increased moisture holding capacity (Kurozawa et al. 2009). As seen in Fig. 1, the particle size distribution of the CSD and USFD-CE samples was mono-modal indicating the fine droplets generated by the atomizing step. Also, the lowest span value of the USFD-CE samples showed that the droplets maintained their size and shape until the end of the process, in agreement with the other studies (Maa et al. 1999; Ishwarya et al. 2015; Wanning et al. 2015). The higher particle size values of USFD samples compared with USFD-CE samples could be explained by the effect of coating materials. The microencapsulation of the enzyme molecules resulted in the formation of larger molecules, and therefore, the particle size and span values of the microencapsulated products were higher than the crude enzyme samples. Although the particle size distributions of the USFD and CFD were similar, there were more agglomerations in increasing particle sizes of CFD samples (Fig. 1).

The obtained powders (USFD-CE, USFD, CFD, and CSD) were analyzed using the BJH method for the surface area, pore volume, and pore size. For this purpose, the porous structure of the samples investigated through nitrogen adsorption-desorption isotherms is illustrated in Fig. 2. The shapes of the isotherms were similar to type IV standard defined by the International Union of Pure and Applied Chemistry for all samples. The type IV isotherms could suggest that the pores of these samples were dominated by micropores (diameter < 2 nm) and mesopores (diameter < 50 nm); however, macropores (diameter > 50 nm) also found to exist since the adsorption isotherm rises rapidly near unity (Gregg and Sing

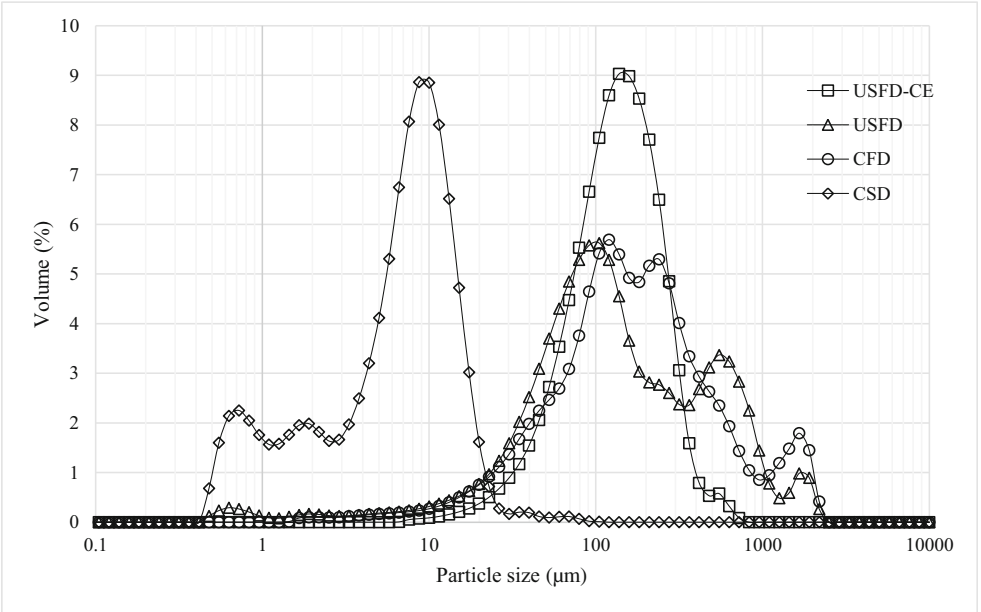


Fig. 1 Particle size distribution of crude and microencapsulated enzymes by different methods

1982). The surface area of the USFD-CE, USFD, CFD, and CSD samples were calculated as 18.97, 1.80, 2.66, and 4.59 m^2/g, respectively. The significant difference ($p < 0.05$) between the crude enzyme and microencapsulated samples demonstrated the effect of microencapsulation on the surface area. Yu et al. (2006) reported that the higher surface area of protein-based materials accelerates protein denaturation due to the increased contact of the particles with air; hence, USFD samples having low surface area were expected

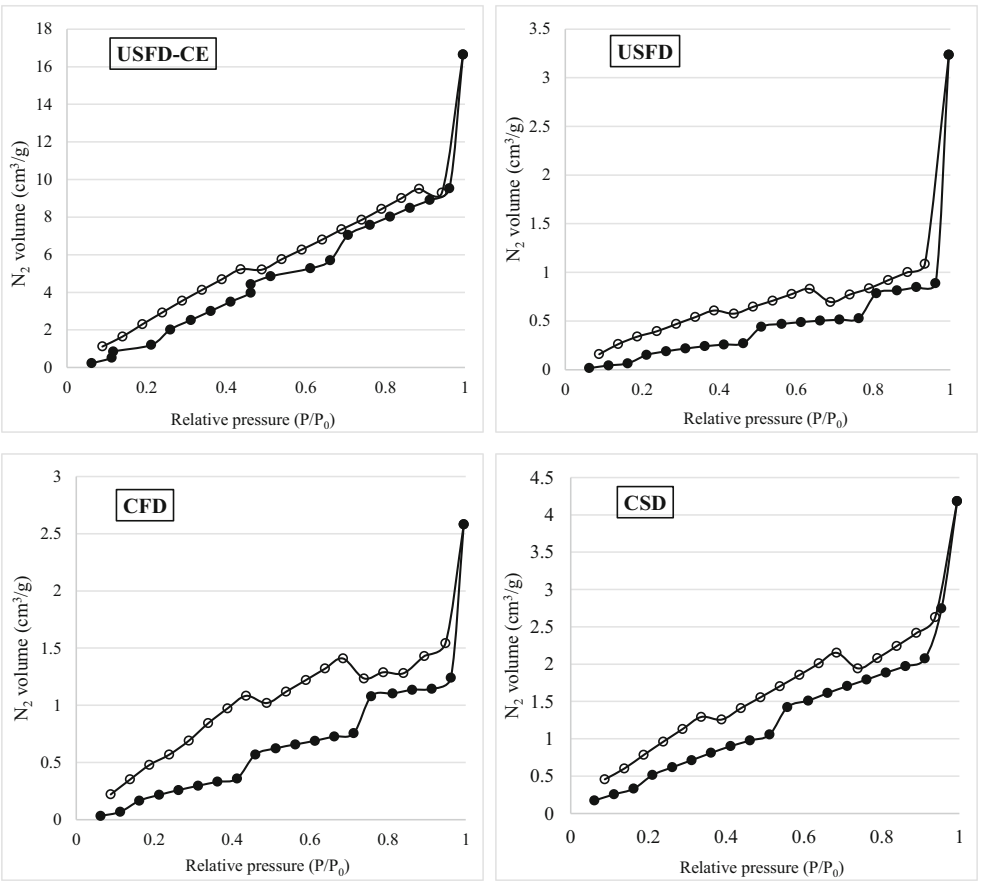


Fig. 2 Adsorption-desorption isotherms of crude and microencapsulated enzymes by different methods. Black-filled circles indicate adsorption. White circles indicate desorption

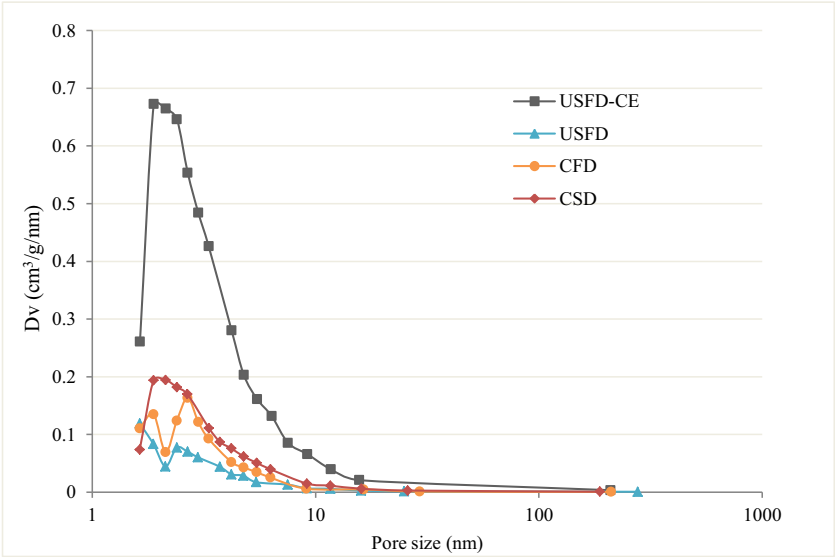


Fig. 3 Pore volume distribution of crude and microencapsulated enzymes by different methods.

to be the most stable ones among all samples. As seen from Fig. 2, all the samples exhibited a hysteresis indicating that there were mesopores and macropores. Also, low-pressure hysteresis was observed which is attributed to the presence of the micropores (Gregg and Sing 1982). De Boer (1958) identified five types of hysteresis loops and correlated them with various pore shapes. According to this classification, type A hysteresis is attributed to cylindrical pores and type B is associated with slit-shaped pores (Labani et al. 2013). It was observed that the pore shape was dominated by the cylindrical pores followed by the slit-shaped pores for the USFD-CE, USFD, and CSD samples, whereas the slit-shaped pores with type B hysteresis were dominant in the CFD samples. The distributions of pore volume with respect to pore size (pore size distribution) of the samples are shown in Fig. 3. According to Fig. 3, a similar pore size distribution was observed between the USFD-CE and CSD samples. A peak at 1.88 nm was observed in the plot for both samples indicating the presence of pores in the microporous range. While most of the pores in the USFD and CFD samples

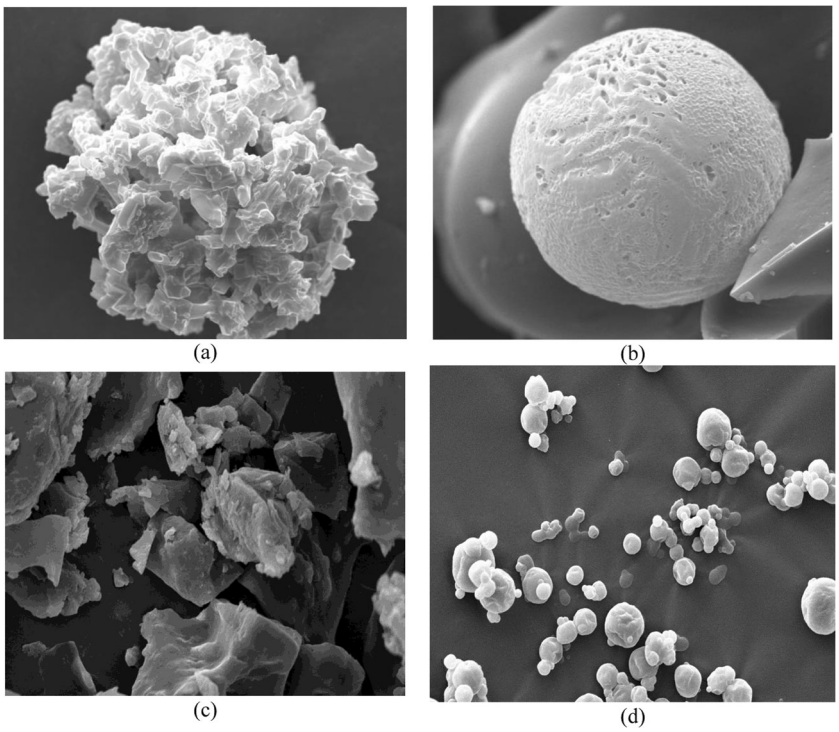


Fig. 4 SEM micrographs of USFD-CE (**a**), USFD (**b**), CFD (**c**), and CSD (**d**). Magnification ratio: 3000×

seemed to be in the mesoporous range (a peak at 2.39 nm for USFD, 2.68 nm for CFD), a steep increase in the volume of pores whose size was smaller than 1.66 nm was observed in the USFD sample (Fig. 3). This indicated that a large quantity of micropores was also present in the USFD samples. The highest pore volume determined in USFD-CE samples could be attributed to the internal pores generated by both ultrasonic atomizing and freeze-drying steps, since the formation of the small ice crystals in fine droplets was followed by sublimation. Hence, some studies in the literature have revealed the porous structure of SFD particles (Constantino et al. 2000; Sonner et al. 2002; Nguyen et al. 2004).

The SEM images showed the morphological differences among the samples (Fig. 4). The USFD-CE particles had sphere-like shapes with irregular and a sponge-like surface, whereas the USFD particles showed more uniform-shaped spheres with a porous surface together with smooth regions. The sponge-like surface of the USFD-CE particles is extremely porous, revealing a network structure of solids interspersed with empty space, and this porous surface structure was covered by microencapsulation as can be seen in the USFD particles (Fig. 4b). Similarly, Niwa et al. (2010) stated that by SEM images they had fluffy and porous powder phenytoin by USFD method; however, this structure was disappeared after usage of coating materials. The CFD samples exhibited irregular and flaky structures, whereas the CSD samples consisted small particles having spherical shapes with small agglomerates (Fig. 4). Although the CSD samples had spherical and smooth surfaces, high temperatures affected the enzyme activity negatively and very small particle size led to an increase in powder agglomeration and caking.

Conclusion

The present study demonstrated that the USFD is an appropriate process to obtain microencapsulated mTG powder with high enzyme activity. Optimization of the USFD conditions was performed and the remaining enzyme activity was maintained at ~ 97%. Furthermore, the microencapsulated samples by USFD were compared with microencapsulated samples by CFD and CSD in terms of microencapsulation efficiency and various physical properties as well as wettability and solubility. Microcapsules with smaller particle size, pore volume, and porosity, with lower moisture content and good reconstitution characteristics, were obtained by USFD with the highest microencapsulation efficiency. Thus, this study indicated that USFD technique could potentially be used for encapsulation of protein-based bioactive materials such as enzymes. However, in the drying stage of the USFD process, operating costs can be increased, especially when conventional freeze drying is required, which requires vacuum application. The USFD process may find application for high value foods containing bioactive molecules, especially when compared with conventional drying methods in terms of the properties of the product obtained. To date, most of the studies related to USFD process are laboratory scale, and hence, scale-up studies are required in this field for the food applications.

Funding Information This study was financially supported by the Scientific and Technological Research Council of Turkey (TUBITAK, Project Number: 115O216) and Tokat Gaziosmanpasa University Scientific Research Projects (Project Number: 2016/62).

References

Aghbashlo, M., Mobli, H., Madadlou, A., & Rafiee, S. (2013). Influence of wall material and inlet drying air temperature on the microencapsulation of fish oil by spray drying. *Food and Bioprocess Technology, 6*(6), 1561–1569.

Allison, S. D., Chang, B., Randolph, T. W., & Carpenter, J. F. (1999). Hydrogen bonding between sugar and protein is responsible for inhibition of dehydration-induced protein unfolding. *Archives of Biochemistry and Biophysics, 365*(2), 289–298.

Amid, M., Manap, Y., & Zohdi, K. N. (2014). Microencapsulation of purified amylase enzyme from pitaya (*hylocereus polyrhizus*) peel in arabic gum-chitosan using freeze drying. *Molecules, 19*, 3731–3743.

Amine, K. M., Champagne, C. P., Salmeri, S., Britten, M., St-Gelais, D., Fustier, P., & Lacroix, M. (2014). Effect of palmitoylated alginate microencapsulation on viability of *Bifidobacterium longum* during freeze-drying. *LWT - Food Science and Technology, 56*, 111–117.

Anchordoquy, T. J., Izutsu, K. I., Randolph, T. W., & Carpenter, J. F. (2001). Maintenance of quaternary structure in the frozen state stabilizes lactate dehydrogenase during freeze–drying. *Archives of Biochemistry and Biophysics, 390*(1), 35–41.

AOAC. (1990). *Official methods for analysis* (15th ed.). Arlington: Association of Official Analytical Chemists.

Bourneow, C., Benjakul, S., & H-Kittikun, A. (2012). Impact of some additives on the stability of microbial transglutaminase from *Providencia sp.* C1112. *Asian Journal of Food and Agro-Industry, 5*(3), 226–233.

Breda, M., Vitolo, M., Duranti, M. A., & Pitombo, R. N. (1992). Effect of freezing-thawing on invertase activity. *Cryobiology, 29*(2), 281–290.

Cano-Chauca, M., Stringheta, P. C., Ramos, A. M., & Cal-Vidal, J. (2005). Effect of the carriers on the microstructure of mango powder obtained by spray drying and its functional characterization. *Innovative Food Science and Emerging Technologies, 6*(4), 420–428.

Carpenter, J. F., & Crowe, J. H. (1989). An infrared spectroscopic study of the interactions of carbohydrates with dried proteins. *Biochemistry, 28*(9), 3916–3922.

Carr, R. L. (1965). Evaluating flow properties of solids. *Chemical Engineering Journal, 72*, 163–168.

Constantino, H. R., Firouzabadian, L., Wu, C., Carrasquillo, K. G., Griebenow, K., Zale, S. E., & Tracy, M. A. (2000). Protein spray freeze drying: effect of formulation variables on particle size and stability. *Journal of Pharmaceutical Science, 17*(11), 1374–1383.

D'Addio, S. M., Chan, J. G. Y., Kwok, P. C. L., Prud'homme, R. K., & Chan, H. K. (2012). Constant size, variable density aerosol particles by ultrasonic spray freeze drying. *International Journal of Pharmaceutics, 427*(2), 185–191.

De Boer, J. H. (1958). The structure and properties of porous materials. In *Proceedings of the Tenth Symposium of the Colston Research Society Held in the University of Bristol* (pp. 68–94). London: Butterworths.

Desai, K. G. H., & Park, H. J. (2005). Recent developments in microencapsulation of food ingredients. *Drying Technology, 23*, 1361–1394.

Dima, C., Pătraşcu, L., Cantaragiu, A., Alexe, P., & Dima, Ş. (2016). The kinetics of the swelling process and the release mechanisms of *Coriandrum sativum L.* essential oil from chitosan/alginate/inulin microcapsules. *Food Chemistry, 195*, 39–48.

Dolly, P., Anishaparvin, A., Joseph, G. S., & Anandharamakrishnan, C. (2011). Microencapsulation of Lactobacillus plantarum (MTCC 5422) by spray-freeze-drying method and evaluation of survival in simulated gastrointestinal conditions. *Journal of Microencapsulation, 28*(6), 568–574.

Eriksson, H. J. C., Hinrichs, W. L. J., van Veen, B., Somsen, G. W., de Jong, G. J., & Frijlink, H. W. (2002). Investigations into the stabilisation of drugs by sugar glasses: I. Tablets prepared from stabilised alkaline phosphatase. *International Journal of Pharmaceutics, 249*(1), 59–70.

Ezhilarasi, P. N., Karthik, P., Chhanwal, N., & Anandharamakrishnan, C. (2013). Nanoencapsulation techniques for food bioactive components: a review. *Food and Bioprocess Technology, 6*(3), 628–647.

Feng, H., Barbosa-Cánovas, G. V., & Weiss, J. (2011). *Ultrasound technologies for food and bioprocessing*. New York: Springer Science and Business Media, 599p.

Furlán, L. T. R., Lecot, J., Padilla, A. P., Campderrós, M. E., & Zaritzky, N. (2012). Stabilizing effect of saccharides on bovine plasma protein: A calorimetric study. *Meat Science, 91*(4), 478–485.

Gaspar, A. L. C., & de Góes-Favoni, S. P. (2015). Action of microbial transglutaminase (MTGase) in the modification of food proteins: A review. *Food Chemistry, 171*, 315–322.

Grasmeijer, N., Stankovic, M., de Waard, H., Frijlink, H. W., & Hinrichs, W. L. (2013). Unraveling protein stabilization mechanisms: vitrification and water replacement in a glass transition temperature controlled system. *BBA Proteins and Proteomics, 1834*(4), 763–769.

Gregg, S. J., & Sing, K. S. W. (1982). *Adsorption, surface area and porosity* (2nd ed.). London: Academic.

Hausner, H. H. (1967). Friction conditions in a mass of metal powder. *Powder Metallurgy, 13*, 7–13.

Heidebach, T., Först, P., & Kulozik, U. (2009). Influence of casein-based microencapsulation on freeze-drying and storage of probiotic cells. *Journal of Food Engineering, 98*, 309–316.

Heinrich, Z. (2003). *Colour chemistry: syntheses, properties and applications of organic dyes and pigments*. Weinheim: Wiley-VCH GmbH & Co. KGaA.

Her, J. Y., Kim, M. S., & Lee, K. G. (2015). Preparation of probiotic powder by the spray freeze-drying method. *Journal of Food Engineering, 150*, 70–74.

Hundre, S. Y., Karthik, P., & Anandharamakrishnan, C. (2015). Effect of whey protein isolate and β-cyclodextrin wall systems on stability of microencapsulated vanillin by spray–freeze drying method. *Food Chemistry, 174*, 16–24.

Ishwarya, S. P., & Anandharamakrishnan, C. (2015). Spray-freeze-drying approach for soluble coffee processing and its effect on quality characteristics. *Journal of Food Engineering, 149*, 171–180.

Ishwarya, S. P., Anandharamakrishnan, C., & Stapley, A. G. F. (2015). Spray-freeze-drying: a novel process for the drying of foods and bioproducts. *Trends in Food Science and Technology, 41*(2), 161–181.

Isleroglu, H., Turker, I., Tokatli, M., & Koc, B. (2018). Ultrasonic spray-freeze drying of partially purified microbial transglutaminase. *Food and Bioproducts Processing, 111*, 153–164.

Jinapong, N., Suphantharika, M., & Jamnong, P. (2008). Production of instant soymilk powders by ultrafiltration, spray drying and fluidized bed agglomeration. *Journal of Food Engineering, 84*(2), 194–205.

Karthik, P., & Anandharamakrishnan, C. (2013). Microencapsulation of docosahexaenoic acid by spray-freeze drying method and comparison of its stability with spray-drying and freeze-drying methods. *Food and Bioprocess Technology, 6*, 2780–2790.

Kumar, R., & Kar, A. (2014). Microencapsulation of nutraceuticals using spray freeze drying method: a brief review. *Indo Global Journal of Pharmaceutical Sciences, 4*(2), 47–51.

Kurozawa, L. E., Morassi, A. G., Vanzo, A. A., Park, K. J., & Hubinger, M. D. (2009). Influence of spray drying conditions on physicochemical properties of chicken meat powder. *Drying Technology, 27*(11), 1248–1257.

Labani, M. M., Rezaee, R., Saeedi, A., & Hinai, A. A. (2013). Evaluation of pore size spectrum of gas shale reservoirs using low pressure nitrogen adsorption, gas expansion and mercury porosimetry: a case study from the Perth and Canning Basins, Western Australia. *Journal of Petroleum Science and Engineering, 112*, 7–16.

Maa, Y. F., Nguyen, P. A., Sweeney, T., Shire, S. J., & Hsu, C. C. (1999). Protein inhalation powders: spray drying vs spray freeze drying. *Pharmaceutical Research, 16*(2), 249–254.

MacLeod, C., McKittrick, J., Hindmarsh, J., Johns, M., & Wilson, D. (2006). Fundamentals of spray freezing of instant coffee. *Journal of Food Engineering, 74*(4), 451–461.

Motoki, M., & Seguro, K. (1998). Transglutaminase and its use for food processing. *Trends in Food Science and Technology, 9*(5), 204–210.

Mujumdar, A. S. (2014). *Handbook of Industrial Drying*. Boca Raton: CRC Press.

Nesterenko, A., Alric, I., Violleau, F., Silvestre, F., & Durrieu, V. (2013). A new way of valorizing biomaterials: the use of sunflower protein for α-tocopherol microencapsulation. *Food Research International, 53*(1), 115–124.

Nguyen, C. X., Herberger, J. D., & Burke, A. D. (2004). Protein powders for encapsulation: a comparison of spray-freeze drying and spray drying of darbepoetin alfa. *Pharmaceutical Research, 21*(3), 507–513.

Niwa, T., Shimabara, H., & Danjo, K. (2010). Novel spray freeze-drying technique using four-fluid nozzle-development of organic solvent system to expand its application to poorly water soluble drugs. *Chemical and Pharmaceutical Bulletin, 58*(2), 195–200.

Pang, Y., Duan, X., Ren, G., & Liu, W. (2017). Comparative study on different drying methods of fish oil microcapsules. *Journal of Food Quality, 2017*, 1–7.

Parthasarathi, S., & Anandharamakrishnan, C. (2016). Enhancement of oral bioavailability of vitamin E by spray-freeze drying of whey protein microcapsules. *Food Bioproducts and Processing, 100*, 469–476.

Popović, L. M., Peričin, D. M., Vaštag, Ž. G., & Popović, S. Z. (2013). Optimization of transglutaminase cross-linking of pumpkin oil cake globulin; improvement of the solubility and gelation properties. *Food and Bioprocess Technology, 6*(4), 1105–1111.

Rajam, R., & Anandharamakrishnan, C. (2015). Microencapsulation of Lactobacillus plantarum (MTCC 5422) with fructooligosaccharide as wall material by spray drying. *LWT-Food Science and Technology, 60*(2), 773–780.

Ramos, A., Raven, N., Sharp, R. J., Bartolucci, S., Rossi, M., Cannio, R., Lebbing, J., Oost, J. V. D., de Vos, W. M., & Santos, H. (1997). Stabilization of enzymes against thermal stress and freeze-drying by mannosylglycerate. *Applied and Environmental Microbiology, 63*(10), 4020–4025.

Ratti, C. (2001). Hot air and freeze-drying of high-value foods: a review. *Journal of Food Engineering, 49*(4), 311–319.

Semyonov, D., Ramon, O., Kaplun, Z., Levin-Brener, L., Gurevich, N., & Shimoni, E. (2010). Microencapsulation of Lactobacillus paracasei by spray freeze drying. *Food Research International, 43*(1), 193–202.

Sonner, C., Maa, Y. F., & Lee, G. (2002). Spray-freeze-drying for protein powder preparation: particle characterization and a case study with

trypsinogen stability. *Journal of Pharmaceutical Sciences, 91*(10), 2122–2139.

Stapley, A. G. F. (2008). Freeze drying. In J. A. Blackwell (Ed.), *Frozen food science technology*. Oxford: Evans.

Sun-Waterhouse, D., Wadhwa, S. S., & Waterhouse, G. I. N. (2013). Spray-drying microencapsulation of polyphenol bioactives: a comparative study using different natural fibre polymers as encapsulants. *Food and Bioprocess Technology, 6*(9), 2376–2388.

Tonnis, W. F., Amorij, J. P., Vreeman, M. A., Frijlink, H. W., Kersten, G. F., & Hinrichs, W. L. J. (2014). Improved storage stability and immunogenicity of hepatitis B vaccine after spray-freeze drying in presence of sugars. *European Journal of Pharmaceutical Sciences, 55*, 36–45.

Tonnis, W. F., Mensink, M. A., de Jager, A., van der Voort Maarschalk, K., Frijlink, H. W., & Hinrichs, W. L. J. (2015). Size and molecular flexibility of sugars determine the storage stability of freeze-dried proteins. *Molecular Pharmaceutics, 12*(3), 684–694.

Turker, I., Domurcuk, G., Tokatli, M., Isleroglu, H., & Koc, B. (2016). Enhancement of microbial transglutaminase production from *Streptomyces sp*. *Ukrainian Food Journal, 5*(2), 306–417.

van Drooge, D. J., Hinrichs, W. L., Dickhoff, B. H., Elli, M. N., Visser, M. R., Zijlstra, G. S., & Frijlink, H. W. (2005). Spray freeze drying to produce a stable Δ9-tetrahydrocannabinol containing inulin-based solid dispersion powder suitable for inhalation. *European Journal of Pharmaceutical Sciences, 26*(2), 231–240.

Wanning, S., Süverkrüp, R., & Lamprecht, A. (2015). Pharmaceutical spray freeze drying. *International Journal of Pharmaceutics, 488*(1), 136–153.

Yu, Z., Johnston, K. P., & Williams, R. O. (2006). Spray freezing into liquid versus spray-freeze drying: influence of atomization on protein aggregation and biological activity. *European Journal of Pharmaceutical Sciences, 27*(1), 9–18.

Zhang, D., Zhu, Y., & Chen, J. (2009). Microbial transglutaminase production: understanding the mechanism. *Biotechnology and Genetic Engineering Reviews, 26*(1), 205–222.

Publisher's Note Springer Nature remains neutral with regard to jurisdictional claims in published maps and institutional affiliations.